Inorg. Chem. **2006**, *45*, 5760–5766

Two 3D Porous Cadmium Tetrazolate Frameworks with Hexagonal Tunnels

Xiang He, Can-Zhong Lu,* and Da-Qiang Yuan

State Key Laboratory of Structural Chemistry, Fujian Institute of Research on the Structure of Matter, Chinese Academy of Sciences, Fuzhou, Fujian 350002, People's Republic of China

Received November 22, 2005

Two novel high-symmetry 3D porous frameworks, $[Cd_5(tetrazolate)_9(OH)(H_2O)]_n \cdot 5nH_2O$ (**1**) and $[Cd_5(5\text{-aminotetrazolate})_9(NO_3)]_n \cdot 3nH_2O$ (**2**), have been synthesized under hydrothermal conditions and characterized by single-crystal X-ray diffraction analysis. The structures of **1** and **2** are characteristic of hexagonal tunnels through the trigonal-prismatic and hexagonal tubelike building units and exhibit their high stabilities of porous frameworks against the removal of the guest molecules.

Introduction

There has been extensive interest in porous metal−organic framework (MOF) materials because of their intriguing molecular topologies and their potential applications in several technological areas, such as gas storage, size-selective separation, molecular recognition, heterogeneous catalysis, and ion exchange.[1−5] The major task of the synthesis for these MOFs is to choose appropriate metal-connecting nodes and/or bridging ligands. Long-bridged ligands or large secondary building units have been used to obtain some porous MOFs. However, crystal structures with such large cavities are stabilized by inclusion of either suitable guests or interpenetrating lattices,[6] and the absence of the guest molecules often results in low thermal stability of the host framework. Consequently, the synthesis of robust open frameworks with both high porosity and thermal stability is still a big challenge for chemists. Tetrazole species are polydentate aromatic N-donor ligand compounds that can act as multidentate bridging ligands and therefore are getting more and more attention.[7] Tetrazolate ligands possess four electron-donating N atoms inducing rich coordination modes with some metal ions, such as Cd^{II}, where the d^{10} configuration and softness of Cd^{II} permit a wide variety of geometries and coordination numbers and may allow one to construct noninterpenetrating high-dimensional structures with good thermal stability. It is worth noting that many MOFs are constructed from the tetrahedral, square, triangular, octahedral, and trigonal-prismatic building blocks;[8−12] however, three-periodic MOF structures based on the assembly of trigonal-prismatic and hexagonal tubelike building units have never been reported before. In this work we have employed tetrazolate ligands with Cd^{II} ions and successfully

* To whom correspondence should be addressed. E-mail: czlu@ms.fjirsm.ac.cn.

(1) (a) Rosi, N. L.; Eckert, J.; Eddaoudi, M.; Vodak, D. T.; Kim, J.; O'Keeffe, M.; Yaghi, O. M. *Science* **2003**, *300*, 1127−1129. (b) Rosi, N. L.; Eddaoudi, M.; Kim, J.; O'Keeffe, M.; Yaghi, O. M. *Angew. Chem., Int. Ed.* **2002**, *41*, 284−287.

(2) (a) Pan, L.; Sander, M. B.; Huang, X.; Li, J.; Smith, M.; Bittner, E.; Bockrath, B.; Johnson, J. K. *J. Am. Chem. Soc.* **2004**, *126*, 1308−1309. (b) Pan, L.; Liu, H.; Kelly, S. P.; Huang, X. Y.; Olson, D. H.; Li, J. *Chem. Commun.* **2003**, 854−855.

(3) (a) Chui, S. S. Y.; Lo, S. M. F.; Charmant, J. P. H.; Orpen, A. G.; Williams, I. D. *Science* **1999**, *283*, 1148−1150. (b) Wu, C. D.; Lin, W. *Angew. Chem., Int. Ed.* **2005**, *44*, 284−287.

(4) Su, C. Y.; Goforth, A. M.; Smith, M. D.; Pellechia, P. J.; Loye, H. C. Z. *J. Am. Chem. Soc.* **2004**, *126*, 3576−3586.

(5) Pschirer, N. G.; Ciurtin, D. M.; Smith, M. D.; Bunz, U. H. F.; Zurloye, H. C. *Angew. Chem., Int. Ed.* **2002**, *41*, 583−586.

(6) Dai, J.-C.; Wu, X.-T.; Fu, Z.-Y.; Hu, S.-M.; Dai, W.-X.; Cui, C.-P.; Wu, L.-M.; Zhang, H.-H.; Sun, R.-Q. *Chem. Commun.* **2002**, 12.

(7) (a) Carlucci, L.; Ciani, G.; Proserpio, D. M. *Angew. Chem., Int. Ed.* **1999**, *38*, 3488−3491. (b) Xiong, R. G.; Xue, X.; Zhao, H.; You, X. Z.; Abrahams, B. F.; Xue, Z. *Angew. Chem., Int. Ed.* **2002**, *41*, 3800−3802. (c) Wang, X. S.; Tang, Y. Z.; Huang, X. F.; Qu, Z. R.; Che, C. M.; Chan, P. W. H.; Xiong, R. G. *Inorg. Chem.* **2005**, *44*, 5278−5285. (d) Tao, J.; Ma, Z. J.; Huang, R. B.; Zheng, L. S. *Inorg. Chem.* **2004**, *43*, 6133−6135. (e) Luo, T. T.; Tsai, H. L.; Yang, S. L.; Liu, Y. H.; Yadav, R. D.; Su, C. C.; Ueng, C. H.; Lin, L. G.; Lu, K. L. *Angew. Chem., Int. Ed.* **2005**, *44*, 2−6. (f) Bronisz, R. *Inorg. Chem. Acta* **2004**, *357*, 396−404.

(8) Ni, Z.; Yassar, A.; Antoun, T.; Yaghi, O. M. *J. Am. Chem. Soc.* **2005**, *127*, 12752−12753.

(9) Kitagawa, S.; Kitaura, R.; Noro, S. I. *Angew. Chem., Int. Ed.* **2004**, *43*, 2334−2375.

(10) Lu, J.; Mondal, A.; Moulton, B.; Zaworotko, M. J. *Angew. Chem., Int. Ed.* **2001**, *40*, 2113−2116.

(11) Livage, C.; Guillou, N.; Chaigneau, J.; Rabu, P.; Drillon, M.; Ferey, G. *Angew. Chem., Int. Ed.* **2005**, *44*, 6488−6491.

(12) (a) Sudik, A. C.; Cote, A. P.; Yaghi, O. M. *Inorg. Chem.* **2005**, *44*, 2998−3000. (b) Eddaoudi, M.; Moler, D. B.; Li, H.; Chen, B.; Reineke, T. M.; O'Keeffe, M.; Yaghi, O. M. *Acc. Chem. Res.* **2001**, *34*, 319−330.

10.1021/ic0520162 CCC: $33.50
Published on Web 06/22/2006

obtained two novel 3D porous frameworks, $[Cd_5(tetrazolate)_9(OH)(H_2O)]_n \cdot 5nH_2O$ (**1**) and $[Cd_5(5\text{-amtta})_9(NO_3)]_n \cdot 3nH_2O$ (**2**, where 5-amtta = 5-aminotetrazolate), with hexagonal channels through the trigonal-prismatic and hexagonal tube-like building units. Both **1** and **2** exhibit high stabilities and maintain their frameworks after removal of the guest molecules.

Experimental Section

Synthesis of $[Cd_5(tetrazolate)_9(OH)(H_2O)]_n \cdot 5nH_2O$ (1). A mixture solution of $Cd(NO_3)_2 \cdot 4H_2O$ (0.31 g, 1 mmol) and tetrazole (0.13 g, 2 mmol) in 20 mL of water was stirred for 20 min at room temperature and then was transferred into a 30-mL Teflon-lined stainless steel vessel. The reaction mixture was heated at 170 °C for 2 days under autogenous pressure. After the reactant was slowly cooled to room temperature, colorless prism-shaped crystals were collected in about 0.11 g (43% yield based on Cd). Anal. Calcd for $C_9H_{22}N_{36}O_7Cd_5$ (1308.63): C, 8.26; H, 1.69; N, 38.53. Found: C, 8.43; H, 1.98; N, 38.62. IR (solid KBr pellet/cm^{-1}): 3431s, 3134m, 1616m, 1456s, 1321m, 1304w, 1221m, 1165s, 1138s, 1097m, 1041m, 1020s, 899w, 692m.

Synthesis of $[Cd_5(5\text{-aminotetrazolate})_9(NO_3)]_n \cdot 3nH_2O$ (2). Compound **2** was synthesized in an procedure analogous to that of **1** except that 5-aminotetrazole (0.17 g, 2 mmol) was used instead of tetrazolate. The reactant mixture was cooled to lead to the formation of colorless prism-shaped crystals of **2** of about 0.10 g (36% yield based on Cd). Anal. Calcd for $C_9H_{24}N_{46}O_6Cd_5$ (1434.74): C, 7.53; H, 1.69; N, 44.91. Found: C, 7.49; H, 1.83; N, 44.62. IR (solid KBr pellet/cm^{-1}): 3442s, 3359m, 3232sh, 1637s, 1556s, 1462m, 1429m, 1385s, 1200m, 1157m, 1086m, 829m, 769m, 586m, 453m, 438m.

Characterization. Elemental analyses of C and H were performed with an EA1110 CHNS-0 CE elemental analyzer. The IR (KBr pellet) spectrum was recorded (400−4000-cm^{-1} region) on a Nicolet Magna 750FT-IR spectrometer. Thermogravimetric analyses (TGA) were carried out in an air atmosphere with a heating rate of 15 °C min^{-1} on a STA449C integration thermal analyzer. Powder X-ray diffraction (XRD) data were collected on a DMAX2500 diffractometer using Cu Kα radiation. The fluorescent data were collected on an Edinburgh FL-FS920 TCSPC system at room temperature.

Structure Determination. Single-crystal XRD data for compounds **1** and **2** were collected on a Rigaku Mercury CCD diffractometer with graphite-monochromated Mo Kα radiation (λ = 0.710 73 Å) at room temperature. The structures were solved by direct methods and refined on F^2 by full-matrix least squares using the *SHELXTL-97* software package.[13] For **1**, the disorder was treated by performing half-occupancies with C and N atoms of the tetrazole ligand. Because of the disorder of the guest and coordination water molecules in the channels, the distribution of these peaks was chemically featureless. Only parts of the guest water molecules have been found in difference Fourier maps. Elemental analysis and TGA showed that each formula unit of compound **1** includes about five guest water molecules. All non-H atoms were refined anisotropically. Crystal data and details of the data collection are given in Table 1. The selected bond distances and angles of compounds **1** and **2** are presented in Table 2.

(13) (a) Sheldrick, G. M. *SHELXS-97, Program for Crystal Structure Solution*; Göttingen University: Göttingen, Germany, 1997. (b) Sheldrick, G. M. *SHELXL-97, Program for Crystal Structure Refinement*; Göttingen University: Göttingen, Germany, 1997.

Table 1. Crystal Data and Structure Refinement for **1** and **2**[a]

compound	**1**	**2**
formula	$C_9H_{22}N_{36}O_7Cd_5$	$C_9H_{24}N_{46}O_6Cd_5$
fw	1308.63	1434.74
cryst size (mm^2)	0.50× 0.38 × 0.30	0.30× 0.10 × 0.08
cryst color	colorless	colorless
cryst syst	hexagonal	hexagonal
Space group	*P*6/*mmm*	$P\bar{6}2c$
a (Å)	26.3397(6)	13.1198(4)
b (Å)	26.3397(6)	13.1198(4)
c (Å)	13.2433(5)	13.6007(7)
V ($Å^3$)	7957.0(4)	2027.43(14)
Z	8	2
θ for data collection (deg)	3.09−27.48	3.49−27.48
reflns collected	60 914	13 637
d_{calcd} (g cm^{-3})	2.108	2.350
T (K)	293(2)	293(2)
wavelength (Å)	0.71073	0.71073
F(000)	4768	1376
abs coeff (mm^{-1})	2.702	2.675
GOF	1.003	1.027
R1, wR2 [$I > 2\sigma(I)$]	0.0842, 0.2661	0.0237, 0.0570
R1, wR2 (all data)	0.0845, 0.2663	0.0239, 0.0572

[a] $R1 = \sum(|F_o| - |F_c|)/\sum|F_o|$; $wR2 = [\sum w(F_o^2 - F_c^2)^2/\sum w(F_o^2)^2]^{0.5}$.

Results and Discussion

Crystal XRD studies[14] reveal that both compounds **1** and **2** have 3D porous structures. In compound **1**, there are five cystallographically independent Cd^{II} ions in an asymmetric unit with distorted octahedral coordination geometries (Figure 1). It is interesting to find four kinds of coordination modes of the tetrazolate ligands all existing together in a compound, and Chart 1 shows their μ_2-tetrazolyl mode (I), two different μ_3-tetrazolyl modes (II and III), and their μ_4-tetrazolyl mode (IV). The skeleton framework consists of a fundamental repeating unit $[Cd_5(tetrazolate)_9(OH)(H_2O)]$, in which each of Cd(1), Cd(2), and Cd(4) is octacoordinated by six tetrazolate ligands in the above-mentioned various coordination modes. The tetrazolate ligands around the Cd centers adopt modes III and IV for Cd(1), adopt four modes (I−IV) for Cd(2), and adopt three modes (II−IV) for Cd(4). Unlike the above Cd ions, Cd(3) is coordinated by one hydroxyl group and five tetrazolate ligands (modes II and III), while Cd(5) links to one water molecule and five tetrazolate ligands (modes III and IV). The Cd−N lengths for Cd(1), Cd(2), and Cd(4) ranging from 2.277(9) to 2.372(6) Å are close to those reported for Cd−N compounds.[7e] Both Cd(3) and Cd(5) centers have a Jahn−Teller compound distorted with four equatorially ligated tetrazoles [Cd(3)−N = 2.341(7) Å; Cd(5)−N = 2.392(8) Å], one axially ligated tetrazole [Cd(3)−

(14) Crystallographic data for **1**: hexagonal, space group *P*6/*mmm* (No. 191), *a* = 26.3397(6) Å, *b* = 26.3397(6) Å, *c* = 13.2433(5) Å, *V* = 7957.0(4) $Å^3$, *Z* = 4, ρ = 2.108 g cm^{-3}, *F*(000) = 4768, μ(Mo Kα) = 2.702 mm^{-1}, GOF = 1.003, of 60 914 total reflections collected, 3466 were unique [*R*(int) = 0.0237], R1 (wR2) = 0.0842 (0.2661) for 203 parameters and 3438 reflections [$I > 2\sigma(I)$]. Crystallographic data for **2**: hexagonal, space group $P\bar{6}2c$ (No. 190), *a* = 13.1198(4) Å, *b* = 13.1198(4) Å, *c* = 13.6007(7) Å, *V* = 2027.43(14) $Å^3$, *Z* = 2, ρ = 2.350 g cm^{-3}, *F*(000) = 1376, μ(Mo Kα) = 2.675 mm^{-1}, GOF = 1.027, of 13 637 total reflections collected, 1617 were unique [*R*(int) = 0.0266], R1 (wR2) = 0.0237 (0.0570) for 111 parameters and 1606 reflections [$I > 2\sigma(I)$]. CCDC-281623 (**1**) and -286210 (**2**) contain the supplementary crystallographic data for this paper. These data can be obtained free of charge at www.ccdc.cam.ac.uk/data_request/cif.

Table 2. Selected Bond Lengths (Å) and Angles (deg) for Compounds **1** and **2**[a]

Compound **1**

Cd(1)−N(15)	2.309(9)	N(15)−Cd(1)−N(8)^{II}	177.4(3)	N(6)−Cd(3)−N(18)	88.74(19)
Cd(1)−N(8)	2.357(8)	N(15)−Cd(1)−N(8)	90.0(2)	O(1)−Cd(3)−N(18)	180.000(2)
Cd(2)−N(10)	2.277(9)	N(8)^{II}−Cd(1)−N(8)	88.1(3)	N(5)−Cd(4)−N(5)^{IV}	88.9(4)
Cd(2)−N(3)	2.344(7)	N(10)−Cd(2)−N(3)	92.6(3)	N(5)−Cd(4)−N(1)^{IV}	178.5(2)
Cd(2)−N(7)	2.368(8)	N(3)−Cd(2)−N(3)^{III}	88.3(4)	N(5)−Cd(4)−N(1)	90.4(3)
Cd(2)−N(16)	2.372(6)	N(10)−Cd(2)−N(7)	179.7(4)	N(5)^{IV}−Cd(4)−N(1)	178.5(2)
Cd(3)−N(6)	2.341(7)	N(3)−Cd(2)−N(7)	87.6(2)	N(1)^{IV}−Cd(4)−N(1)	90.3(4)
Cd(3)−O(1)	2.350(19)	N(3)−Cd(2)−N(16)^{III}	91.3(3)	N(5)−Cd(4)−N(13)	91.4(3)
Cd(3)−N(18)	2.403(13)	N(3)^{III}−Cd(2)−N(16)^{III}	176.4(2)	N(1)−Cd(4)−N(13)	89.9(3)
Cd(4)−N(5)	2.330(7)	N(10)−Cd(2)−N(16)	91.0(3)	N(5)−Cd(4)−N(19)^{I}	88.3(2)
Cd(4)−N(1)	2.327(7)	N(3)−Cd(2)−N(16)	176.4(2)	N(1)−Cd(4)−N(19)^{I}	90.4(2)
Cd(4)−N(13)	2.344(9)	N(3)^{III}−Cd(2)−N(16)	91.3(3)	N(13)−Cd(4)−N(19)^{I}	179.5(3)
Cd(4)−N(19)^{I}	2.368(10)	N(7)−Cd(2)−N(16)	88.8(2)	N(2)−Cd(5)−N(2)^{VI}	177.0(4)
Cd(5)−N(2)	2.392(8)	N(6)^{IV}−Cd(3)−N(6)	88.6(4)	N(2)−Cd(5)−N(2)^{IV}	90.0(4)
Cd(5)−N(12)	2.412(18)	N(6)^{I}−Cd(3)−N(6)	91.4(4)	N(2)^{IV}−Cd(5)−N(2)^{IV}	89.9(4)
Cd(5)−O(2)	2.39(6)	N(6)−Cd(3)−N(6)^{V}	177.5(4)	N(2)−Cd(5)−N(12)	88.5(2)
N(15)^{II}−Cd(1)−N(15)	91.7(3)	N(6)−Cd(3)−O(1)	91.26(19)	N(2)−Cd(5)−O(2)	91.5(2)
				N(12)−Cd(5)−O(2)	180.000(2)

Compound **2**

Cd(1)−N(6)^{I}	2.345(3)	N(6)^{I}−Cd(1)−N(3)	177.75(15)	N(5)^{II}−Cd(2)−N(7)	177.79(17)
Cd(1)−N(3)	2.356(3)	N(6)^{II}−Cd(1)−N(3)	89.79(14)	N(7)−Cd(2)−N(7)^{III}	88.6(2)
Cd(2)−N(5)^{II}	2.331(4)	N(6)^{III}−Cd(1)−N(3)	92.22(14)	N(5)^{V}−Cd(2)−N(2)	90.45(14)
Cd(2)−N(7)	2.343(4)	N(3)^{IV}−Cd(1)−N(3)	90.02(10)	N(5)^{II}−Cd(2)−N(2)	90.10(14)
Cd(2)−N(2)	2.380(3)	N(5)^{V}−Cd(2)−N(5)^{II}	92.3(2)	N(7)−Cd(2)−N(2)	88.67(14)
N(6)^{I}−Cd(1)−N(6)^{II}	87.98(12)	N(5)^{V}−Cd(2)−N(7)	89.53(12)	N(7)^{III}−Cd(2)−N(2)	90.76(13)
				N(2)−Cd(2)−N(2)^{III}	179.2(2)

[a] Symmetry transformations used to generate equivalent atoms: (I) $x, y, -z + 1$, (II) $-x + y, -x + 1, z$, (III) $-x + y, y, z$, (IV) $-x, -x + y, z$, (V) $-x, -x + y, -z + 1$, and (VI) $-x, -x + y, -z$ for **1**; (I) $x - y + 1, -y + 1, -z + 1$, (II) $-x + 1, -x + y, -z + 1$, (III) $y, x, -z + 1$, (IV) $-y + 1, x - y, z$, and (V) $-x + y, -x + 1, z$ for **2**.

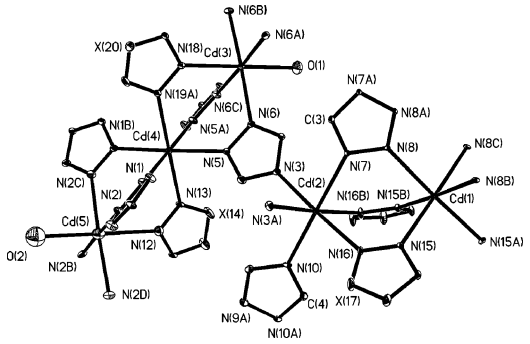

Figure 1. ORTEP drawing showing the coordination of Cd ions in compound **1**.

Chart 1. Four Kinds of Coordination Modes for Tetrazolate Ligands (R = H or NH_2) in **1**

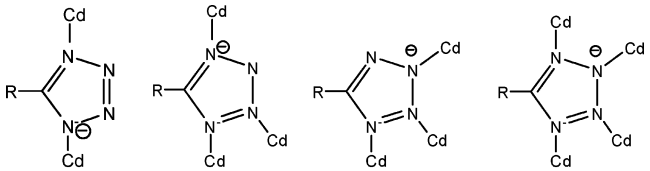

N(18) = 2.403(13) Å; Cd(5)−N(12) = 2.412(18) Å], and one axial hydroxyl group or water molecule [Cd(3)−O(1) = 2.350(19) Å; Cd(5)−O(2) = 2.39(6) Å; Figure S1 in the Supporting Information].

The structure of **1** is built up by two kinds of building blocks, one that can be viewed as a hexagonal tube with pores in dimensions of approximately 8.371 Å × 8.371 Å (block **A**) and the other as a trigonal prism (block **B**). Blocks **A** and blocks **B** connect to each other using Cd(2) atoms as their common vertexes. Viewed along the *c* axis, it can be found out that each of blocks **A** shares six vertexes with six adjacent blocks **B** and each of blocks **B** shares all vertexes with three blocks **A**. Moreover, six blocks **A** and six blocks **B** all use one side to form a big 54-membered ring, which contains 9 Cd(3) atoms, 9 Cd(2) atoms, and 18 tetrazolate ligands (Figure S2 in the Supporting Information). Each ring intersected with six other adjacent rings to form a 2D mosaic layer network (Figure 2c). Building block **A** is constructed by Cd(5), Cd(4), Cd(3), and Cd(2) atoms bridged by tetrazolate ligands. From the *b* axis, it can be seen that there are 6 Cd(5), 12 Cd(4), and 12 μ_4-tetrazolate ligands to form a crown with the hexagonal pores (Figure S3 in the Supporting Information). Cd(4), Cd(3), and Cd(2) atoms are connected by μ_3-tetrazolate ligands (mode II), while μ_3-tetrazolate ligands (mode III) bridged Cd(4) and Cd(5) or Cd(3) and Cd(4) to form block **A**. The blocks **A** connect each other to form the 1D hexagonal channel (unit **C**; Figure 2a). Block **B** is made up of Cd(1) and Cd(2) with the tetrazolate ligands. Cd(1) atoms locate at the threefold axis, and there is one mirror between the adjacent Cd(1) atoms. Through three μ_3-tetrazolate ligands (mode III), the three Cd(2) atoms not only connect with each other but also further link to Cd(1) atoms. Three μ_4-tetrazolate ligands bridge two mirror symmetrical Cd(1) atoms and two mirror symmetrical Cd(2) atoms, while three μ_2-tetrazolate ligands bridge the Cd(2) atoms and other Cd(2) from the next block **B**. The blocks **B** connect to each other to form the 1D trigonal prism (unit **D**; Figure 2b). Such units **C** and **D** are connected together by Cd(2) atoms and bridging tetrazolate ligands to form an interesting 3D porous framework (Figures 2d,e and S4 in the Supporting Information). To the best of our

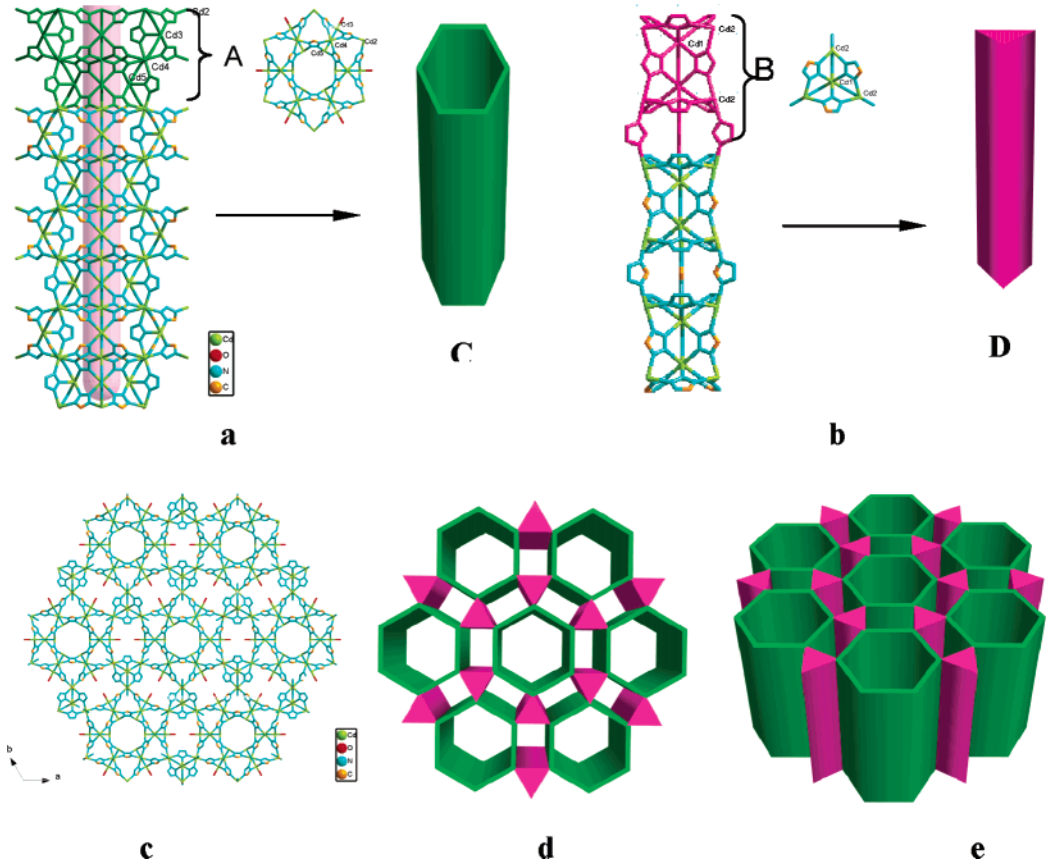

Figure 2. (a) Hexagonal channel **C** made by building blocks **A** viewed along the *b* axis. (b) Trigonal prism **D** made by building block **B**. The H atoms and water molecules are omitted for clarity. (c) 2D layer structure of **1** viewed along the *c* axis. The H atoms and water molecules are omitted for clarity. (d) Perspective view of compound **1** viewed along the *c* axis. (e) Perspective view of the 3D structure of compound **1**.

knowledge, this particular type of network composed of hexagonal channel **C** and trigonal prism **D** sharing common vertexes has never been reported before. It is also worth noting that compound **1** is the first coordination polymer of a *P*6/*mmm* space group constructed by transition-metal and organic ligands.[15] Calculations using PLATON[16] show that the effective volume for the inclusion is about 1935.1 Å^3 per unit cell, comprising 24.3% of the crystal volume of **1**.

Compound **2** crystallizes in the high-symmetry hexagonal noncentrosymmetric space group $P\bar{6}2c$, with two crystallographically independent Cd^{II} ions in the asymmetric unit with distorted octahedral coordination geometries (Figure 3). The 5-amtta ligands around Cd centers adopt modes III and IV for Cd(1) and Cd(2) (Figure S5 in the Supporting Information). In contrast to compound **1**, the structure of **2** is built up only by the trigonal-prism blocks **B**, using Cd(2) atoms as their common vertexes to connect to each other. Viewed along the *c* axis, it can be seen that such blocks **B** share three vertexes with three adjacent blocks **B** to form the 2D layer structure with pores in dimensions of approximately 6.089 Å × 6.089 Å (Figure 5a). From the *b* axis, similar to compound **1**, the blocks **B** in **2** connect each other to form the 1D trigonal prism **D** units, and the difference is that the coordination mode of three 5-amtta ligands in the **B** building

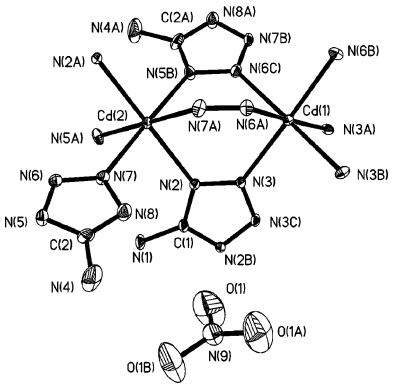

Figure 3. ORTEP drawing showing the coordination of Cd ions in compound **2**.

block adopted a μ_4 bridge instead of a μ_2 bridge in compound **1** (Figure 4). As a result, such a trigonal prism **D** is connected together by Cd(2) atoms and bridging tetrazolate ligands to form a 3D porous cationic framework with nitrate anions and guest water molecules filled in the channels (Figures 5b,c and S6 in the Supporting Information). The presence of nitrate anions in the open channels of **2** is also supported by the IR spectrum, which exhibits an intense peak at around 1385 cm^{-1} for the N−O stretches. Intramolecular H-bonding interactions between the N atom of the amino group and the O atom of nitrate ion N(4)−H(8B)···O(1) [$-x$, $-x + y$, $-1/2 + z$; 3.126(17) Å] and the O atom of water N(4)−

(15) Cambridge Crystallographic Database ConQuest, version 1.7.
(16) Spek, A. L. *PLATON, A Multipurpose Crystallographic Tool*; Utrecht University: Utrecht, The Netherlands, 2001.

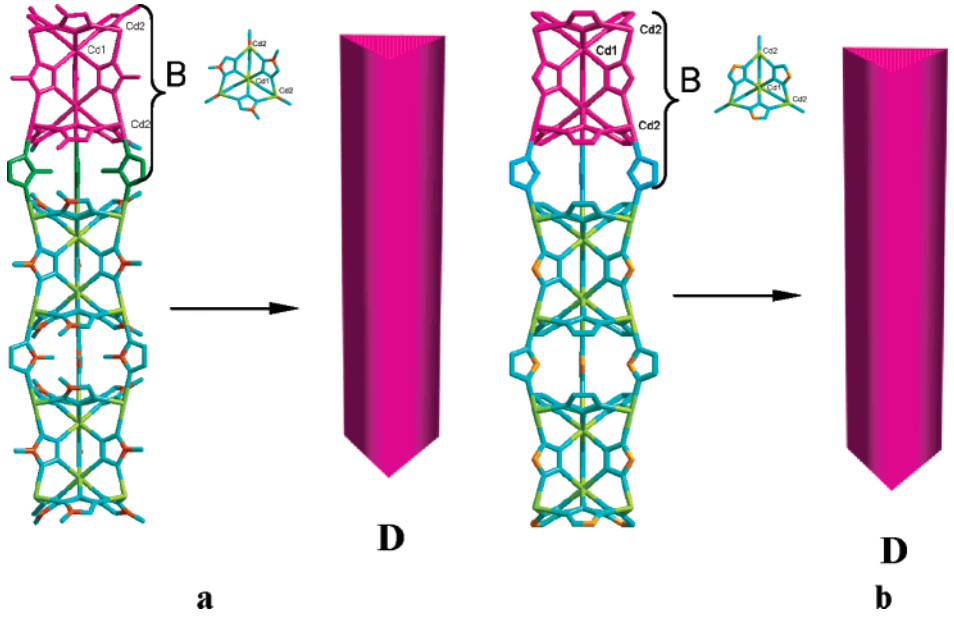

Figure 4. (a) Trigonal prism **D** formed by building block **B** in compound **2**. Compared to compound **1**, the coordination mode of three 5-amtta ligands (in green color) adoped a μ_4 bridge instead of a μ_2 bridge tta ligand (in blue color) in compound **1**. (b) Trigonal prism **D** formed by building block **B** in compound **1**. The H atoms are omitted for clarity.

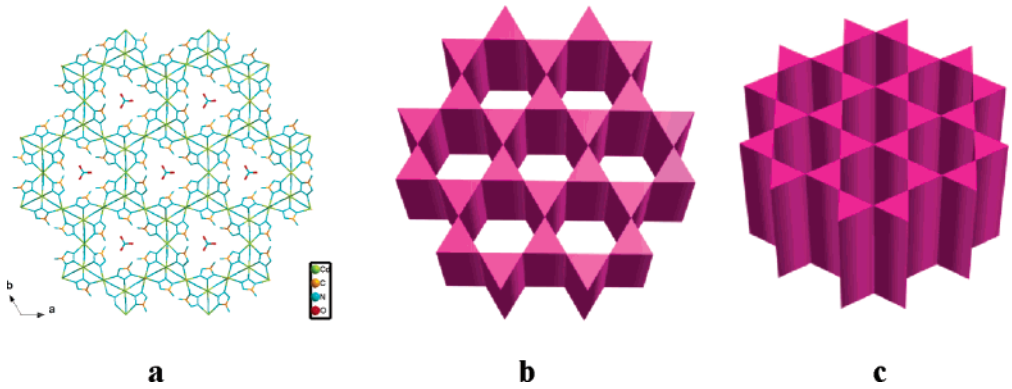

Figure 5. (a) 2D layer structure of **2** viewed along the *c* axis. The H atoms and water molecules are omitted for clarity. (b) Perspective view of compound **2**, showing the hexagon pores. (c) Perspective view of the 3D structure of compound **2**.

H(8A)···O(1W) [*y*, *x*, −*z*; 2.930(19) Å] exist in compound **2**. As a result, nitrate anions and guest water molecules are all located in the channel steadily, which can be proven by the TGA data. PLATON shows that the effective volume for the inclusion is about 417.0 Å^3 per unit cell, comprising 20.6% of the crystal volume of **2**. The structure of **2** is related to the "kag" net (Figure 5b), the 3D equivalent of the well-known 2D [3.6.3.6] kagome net, while compound **1** is related to another semiregular plane net [3.4.6.4] observed as a pattern of the anions in the hexagonal tungsten bronze and in the $BaSiF_6$ structure.[17]

Compounds **1** and **2** are insoluble in common organic solvents and water. Two porous frameworks both exhibit high robustness and thermal stability. The TGA curve indicates that a weight loss of 8.46% occurred in the temperature range of 30−200 °C, corresponding to the loss of five guest molecules and one coordinated water molecule for **1** (expected 8.26%) and that a weight loss of 4.03% occurred in the temperature range of 30−180 °C, corresponding to the loss of three guest water molecules for **2** (expected 3.77%). Then, no further weight loss was observed until 280 °C for **1** or 300 °C for **2** (Figures 6 and 7). To study their dehydrated frameworks with the powder XRD technique, samples of **1** and **2** were evacuated at 150 °C for 24 h under vacuum, and the XRD patterns of the resultant solid show the main reflections remaining unaltered as the pristine samples of **1** and **2**, indicating that the framework structures of **1** and **2** are maintained after complete removal of the water molecules (Figures S7 and S8 in the Supporting Information). To further test the thermal stability of compounds **1** and **2**, heating−cooling experiments were carried out according to the TGA results and monitored by XRD. Compared to the XRD data for the original crystals of **1** and **2**, as shown in Figures 8 and 9, the XRD patterns for **1** and **2** at 240 °C in air remained unchanged, indicating that the

(17) (a) Delgado-Friedrichs, O.; Foster, M. D.; O'Keeffe, M.; Proserpio, D. M.; Treacy, M. M. J.; Yaghi, O. M. *J. Solid State Chem.* **2005**, *178*, 2533−2554. (b) Ockwig, N. W.; Delgado-Friedrichs, O.; O'Keeffe, M.; Yaghi, O. M. *Acc. Chem. Res.* **2005**, *38*, 176−182.

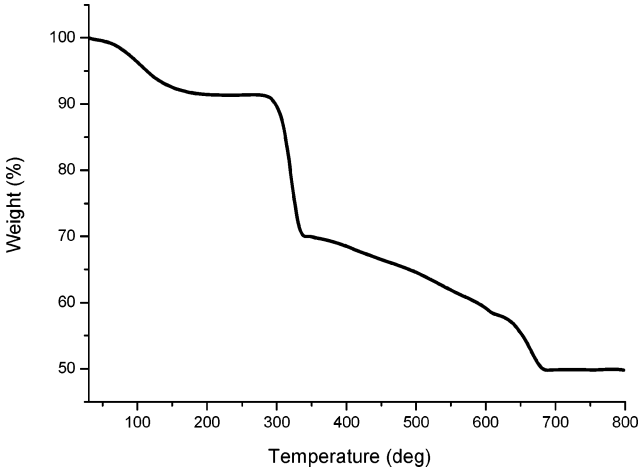

Figure 6. Plot of TGA curves for **1** under an air atmosphere.

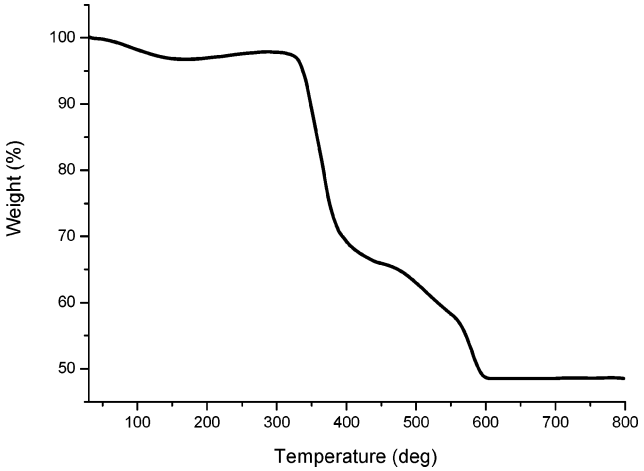

Figure 7. Plot of TGA curves for **2** under an air atmosphere.

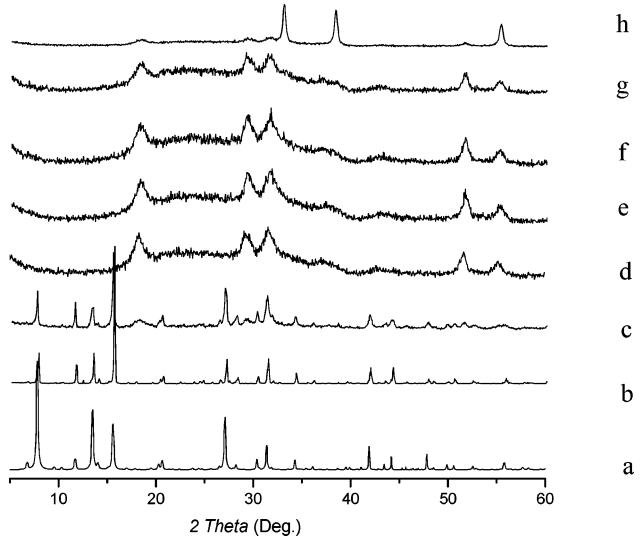

Figure 8. XRD patterns for **1** (a) calculated on the basis of the structure determined by single-crystal XRD, (b) taken at room temperature, (c) taken after heating at 240 °C for 30 min, (d) taken after heating at 280 °C for 30 min, (e) taken after heating at 300 °C for 30 min, (f) taken after heating at 330 °C for 30 min, (g) taken after heating at 360 °C for 30 min, and (h) taken after heating at 430 °C for 30 min.

structural integrities of the frameworks are maintained. When the samples were heated to 280 °C, the XRD pattern of **1** changed completely, revealing the collapse of the framework,

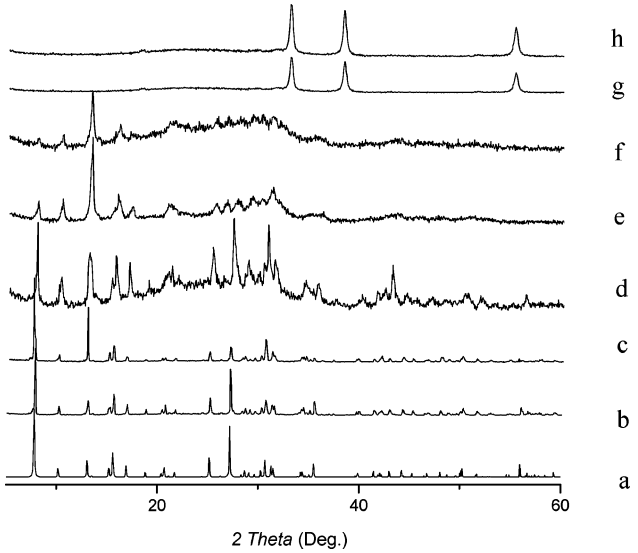

Figure 9. XRD patterns for **2** (a) calculated on the basis of the structure determined by single-crystal XRD, (b) taken at room temperature, (c) taken after heating at 240 °C for 30 min, (d) taken after heating at 280 °C for 30 min, (e) taken after heating at 300 °C for 30 min, (f) taken after heating at 330 °C for 30 min, (g) taken after heating at 360°C for 30 min, and (h) taken after heating at 430 °C for 30 min.

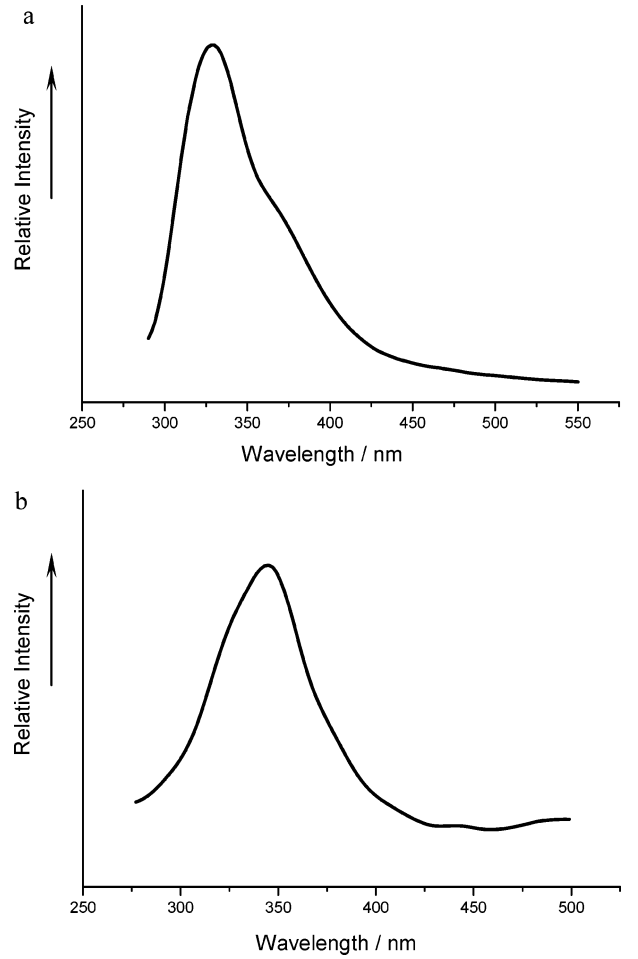

Figure 10. (a) Emission spectrum of compound **1** measured in the solid state at room temperature. (b) Emission spectrum of compound **2** measured in the solid state at room temperature.

while **2** began a structural transformation at 300 °C; the XRD pattern of **2** changed completely at 330 °C, revealing the

collapse of the framework. When the samples were heated at 380 °C, the XRD pattern of **2** showed a new crystalline phase formed in good agreement with CdO, while at 430 °C, the XRD pattern of **1** showed results similar to those of **2** to form the CdO.

The photoluminescent properties for compounds **1** and **2** are also investigated in the solid state. It can be observed that both compounds **1** and **2** exhibit photoluminescence upon photoexcitation at 280 and 275 nm, respectively. The emission peaks at 330 nm for **1** and 347 nm for **2** are attributed to intraligand ($\pi-\pi^*$) fluorescence (Figure 10) because a very weak similar emission with λ_{max} at 328 nm is also observed for the free ligand.

Conclusion

In conclusion, two nanotubular 3D MOFs, **1** and **2**, have been constructed under hydrothermal conditions from Cd salts and multidentate tetrazole as a bridging ligand. These remarkable topologies of 3D porous structures with hexagonal channels are composed of the novel building units, hexagonal channel **C**, and trigonal prism **D**, which might provide some useful information for the construction of new frameworks. XRD studies confirm that the pore frameworks of **1** and **2** exhibit high stabilities against the removal of the guest molecules with thermal conditions. These studies highlight an intriguing feature of coordinative network chemistry in producing rich architectures and topologies and bring a new member to the family of suprastructures.

Acknowledgment. Special thanks are offered to reviewer 1 for pointing out the topology structures of compounds **1** and **2**. This work was supported by the 973 program of the MOST (Grant 001CB108906), the National Science Foundation of China Science Foundation of China (Grants 20425313, 90206040, 20333070, and 20303021), the National Science Foundation of Fujian, and Chinese Academy of Sciences.

Supporting Information Available: Complete descriptions of the X-ray single-crystal structural collection and analysis, details of experiment, ORTEP representation, and other structure drawings, TGA, and XRD patterns of **1** and **2**. This material is available free of charge via the Internet at http://pubs.acs.org.

IC0520162